ON THE EFFICIENCY OF ANALYZING 3D ANISOTROPIC, TRANSVERSELY ISOTROPIC, AND ISOTROPIC BODIES IN BEM

Y. C. Shiah [*] **W. X. Sun** [**]

Department of Aerospace and Systems Engineering
Feng Chia University
Taichung, Taiwan 40724, R.O.C.

ABSTRACT

Due to a lack of closed-form solutions for three dimensional anisotropic bodies, the computational burden of evaluating the fundamental solutions in the boundary element method (BEM) has been a research focus over the years. In engineering practice, transversely isotropic material has gained popularity in the use of composites. As a degenerate case of the generally anisotropic material, transverse isotropy still needs to be treated separately to ease the computations. This paper aims to investigate the computational efficiency of the BEM implementations for 3D anisotropic, transversely isotropic, and isotropic bodies. For evaluating the fundamental solutions of 3D anisotropy, the explicit formulations reported in [1,2] are implemented. For treating transversely isotropic materials, numerous closed form solutions have been reported in the literature. For the present study, the formulations presented by Pan and Chou [3] are particularly employed. At the end, a numerical example is presented to compare the computational efficiency of the three cases and to demonstrate how the CPU time varies with the number of meshes.

Keywords : Boundary element method, Transversely isotropic, 3D anisotropic.

1. INTRODUCTION

The boundary element method has been renowned for its distinctive feature that only the boundary of a physical domain needs to be modeled. In recent years, BEM has received popularity due to its easily modeling of engineering problems. However, the development of an efficient BEM algorithm for the elastostatics analysis of 3D generally anisotropic bodies can hardly keep pace with the same analysis for isotropy. For analysis of isotropic elastostatics, the fundamental solutions can be expressed in relatively simple forms and, therefore, the computational effort has not been a serious issue. This is also the case for 2D anisotropic elastostatics; however the same does not hold true for 3D general anisotropy. The principal impediment lies in the mathematical complexity of its fundamental solutions that lead to computational burden to evaluate them. Due to this reason, their numerical evaluation has remained a subject of research, particularly in the BEM community.

The derivation for the fundamental solutions of 3D generally anisotropic medium can be traced a long way back to reference [4], where the displacement field was expressed as a line integral around a unit circle with integrand containing the Christoffel matrix defined in terms of elastic constants. In the past decades, researchers have been dedicated to simplifying of this integral as well as developing computationally efficient schemes (*e.g.* [5-9]). Employing the Radon transform and the calculus of residues, Wang [10] derived an explicit expression for the displacement Green's function which involved contour integration over a rectangular parallelepiped. Following his work, Tonon *et al*. [11] implemented it in a BEM formulation. Recently, Wang and Denda [12] have also presented a BEM algorithm for 3D generally anisotropic elasticity, where the Green's function for displacements is expressed in terms of a contour integral over a semi-circle. Analytical solution of the integral is obtained over triangular boundary elements with piecewise linear interpolation function in their BEM implementation. Claiming it to be the most explicit form, Ting and Lee [1] derived the displacement fundamental solution, based on Stroh's formalism. The formulation, primarily expressed in terms of Stroh's eigenvalues, is much simpler in form than that obtained by Wang [10] and still remains valid for repeated eigenvalues. Lee [2] further derived the analytical expressions for the derivatives of Green's displacements for up to second order. Further, Tan *et al*. [13] implemented the algorithm into an existing BEM code, based on quadratic isoparametric elements, yet no discussion about its computational efficiency was addressed.

Characterized by different material symmetries, some special cases of practical interest, such as the

[*] Professor, corresponding author [**] Research associate

monoclinic material, orthotropic material, and transversely isotropic material, have attracted great amounts of researches in the past. From the characterized material symmetry, the number of elastic constants of each respective case can be significantly reduced. Due to the relative simplicity, the fundamental solutions of these particular cases are expected to share a similar computational efficiency. Among such material configurations, transverse isotropy, as illustrated by hexagonal systems [14,15], is probably of the most interest due to its extensive applications in the community of composites. For this, the transversely isotropic material is particularly chosen as the subject for the present investigation. One of the earliest studies for transverse isotropy is contributed by Michell [16], solving the elastostatics problem of a half-space transversely isotropic body subjected to surface tractions. Hu [17] considered the general case of elastostatics problem in transversely isotropic media and generalized Lekhnitskii's solution. Since then, many studies on transverse isotropy have appeared (*e.g.* [18-25]). Recently, Chen *et al.* [26] have analytically derived the Green's functions of biharmonic problems with circular and annular domains. Among pertinent works in this regard, the fundamental solution proposed by Pan and Chou [3] is particularly chosen and implemented in BEM for our present study. This choice can be attributed to two major reasons. One is due to the straightforwardness of the form, and the other is the fact that the formulation can be further utilized to perform the volume integral transformation [27] for the problem of thermoelasticity in BEM. This exact transformation has never been reported in the open literature yet. As the groundwork of such treatment for our future research, the formulation [3] is employed for the present study.

For verifying our BEM implementation of the transversely isotropic formulation, a few numerical examples are investigated that the transverse isotropy is intentionally treated as a particular case of general anisotropy. By numerical experiments for increased meshes, the CPU time and also the accuracy of the both approaches can be analyzed for their computational efficiencies.

2. BOUNDARY INTEGRAL EQUATION FOR 3D ISOTROPIC ELASTOSTATICS

As is well established in the BEM literature, the direct formulation of BEM for 3D isotropic solids relates the displacements u_i and the tractions t_i of the source point P and the field point Q on the boundary S by the following integral equation,

$$C_{ij}(P)\,u_i(P) + \int_S u_i(Q)\,T_{ij}(P,Q)\,dS = \int_S t_i(Q)\,U_{ij}(P,Q)\,dS + \int_V B_i(q)\,U_{ij}(P,q)\,dV\ , \qquad (1)$$

where q is an arbitrary field point inside the domain volume V; B_i is used to denote an equivalent body-force component such as the thermal and inertia effect. In Eq. (1), U_{ij} and T_{ij} are the fundamental solutions for displacements and tractions, respectively. For 3D isotropic medium, they are written in terms of the radial distance between the source and the field point, denoted by r, as

$$U_{ij} = \frac{\left[(3-4\nu)\,\delta_{ij} + r_{,i}\,r_{,j}\right]}{16\,\pi\,\mu\,(1-\nu)\,r}, \qquad (2a)$$

$$T_{ij} = \frac{-\left\{(dr/dn)\left[(1-2\nu)\,\delta_{ij} + 3\,r_{,i}\,r_{,j}\right] + (1-2\nu)(r_{,i}\,n_j - r_{,j}\,n_i)\right\}}{8\,\pi(1-\nu)\,r^2}, \qquad (2b)$$

where δ_{ij} is the Kronecker Delta defined as usual, n_i is the component of the unit outward normal vector, ν and μ are the Poisson's ratio and the shear modulus, respectively. Details of the derivation can be referred to [28]. It is obvious that no issues of computational efficiency will arise upon the straightforwardness of these formulations for isotropy. However, this cannot be said for those of anisotropy that will be elaborated later on. Herein, a few more details about the body-force term in Eq. (1) may be probably worth explaining a little since this regards the justification of our use of the fundamental solutions provided by Pan and Chou [3] for transverse isotropy. For the problem of thermoelasticity, the boundary integral equation becomes

$$C_{ij}(P)\,u_i(P) + \int_S u_i(Q)\,T_{ij}(P,Q)\,dS = \int_S t_i(Q)\,U_{ij}(P,Q)\,dS + \int_S \gamma_{ik}\,n_k\Theta U_{ij}(P,Q)\,dS - \int_V \gamma_{ik}\,\Theta_{,k}U_{ij}(P,q)\,dV\ , \qquad (3)$$

where γ_{ik} are thermal moduli and Θ is the temperature change. Obviously, computation of the extra volume integral in Eq. (3) will conventionally require domain discretization that destroys the BEM's distinctive notion of boundary discretization. To restore the BEM's notion, the volume integral needs to be transformed into boundary ones as described in [27]. The key to the success of such transformation lies in the use of the Green's Theorem and a process to determine the new fundamental solution G_{ijk} that satisfies

$$\nabla^2 G_{ijk} = U_{ij,k}\ , \qquad (4)$$

where the operator ∇^2 stands for the Laplacian operation and "$,k$" in the subscript index is used to denote the spatial differentiation in the k-direction. This process of exact volume-to-surface transformation has been widely used in isotropic elasticity. The major impediment of such transformation for 3D anisotropy is derived from its mathematical complexity of the Green's displacement field. On the same account, similar transformation for 3D transverse isotropy has not been successful so far. For transverse isotropy, the fundamental solution derived by Pan and Chou [3] is implemented; for generally anisotropy, the one by Lee [2] is used.

3. FUNDAMENTAL SOLUTIONS OF GENERAL 3D ANISOTROPY

An efficient scheme to evaluate these Green functions is important for the development of a robust and successful computational tool for the stress analysis of 3D elastic solids. As presented previously for 3D isotropy, the fundamental solutions, given in Eq. (2a) and (2b), will not pose any problem leading to concerns for computation inefficiency. Due to a lack of closed forms, the fundamental solutions of 3D anisotropy have been a focus of research in the BEM community. Many solutions have been proposed in different forms over the years, but none of them has demonstrated the CPU computation time and compared with isotropic cases when implemented in BEM. For the present study, we employ the closed form solutions derived by Ting and Lee [1] for the displacement and those derived by Lee [2] for the displacement derivatives. Implementation of these formulations in BEM has been presented by Tan *et al*. [13]. For completeness, the formulations are briefed herein and more details may be referred to [13].

As shown in Fig. 1, suppose a field point P is defined by the local spherical coordinates (r, θ, ϕ) when the source point Q is settled at the origin. The vectors **n**, **m** along with **x**/r form a right-handed triad [**n**, **m**, **x**/r]. The general form of **n** and **m** can be expressed as

$$\begin{aligned} \mathbf{n} &= (\cos\phi\cos\theta\ ,\ \cos\phi\sin\theta\ ,\ -\sin\phi)\ , \\ \mathbf{m} &= (-\sin\theta\ ,\ \cos\theta,\ 0)\ . \end{aligned} \tag{5}$$

As a result, one may obtain a sextic equation in p by setting the determinant of the matrix $\mathbf{\Gamma} = |\mathbf{Q} + p(R + R^T) + p^2 T|$ to be null, where **Q**, **R**, **T** are given by

$$Q_{ik} = C_{ijks}\, n_j\, n_s,\ R_{ik} = C_{ijks}\, n_j\, m_s,\ T_{ik} = C_{ijks}\, m_j\, m_s\ , \tag{6}$$

and C_{ijks} are the stiffness coefficients of the anisotropic material with 21 independent constants. The six roots of the sextic equation are the Stroh eigenvalues; they must be complex for the strain energy to be positive and they appear as three pairs of complex conjugates, expressed as

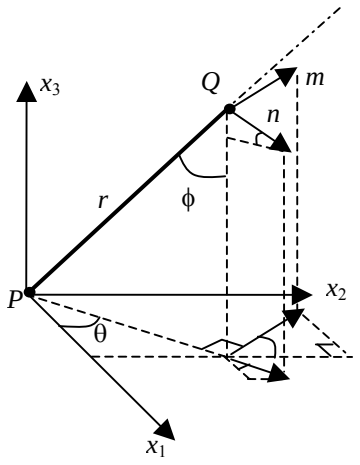

Fig. 1 Definition of the unit vectors **n**, **m**

$$p_\nu = \alpha_\nu + i\,\beta_\nu\ ,\ \beta_\nu > 0\ ,\ (\nu = 1,\ 2,\ 3)\ . \tag{7}$$

Eventually, the displacement field is given by

$$\mathbf{U}(\mathbf{x}) = \frac{1}{4\pi r}\mathbf{H}\,[\mathbf{x}]\ , \tag{8}$$

where **H**[**x**], called the Barnett-Lothe tensor, is defined by

$$H[x] = \frac{1}{|T|}\sum_{n=0}^{4} q_n\,\hat{\Gamma}^{(n)}\ , \tag{9}$$

In Eq. (9), $\hat{\mathbf{\Gamma}}^{(n)}$ is given by

$$\hat{\Gamma}_{ij}^{(n)} = \tilde{\Gamma}_{(i+1)(j+1)(i+2)(j+2)}^{(n)} - \tilde{\Gamma}_{(i+1)(j+2)(i+2)(j+1)}^{(n)}\ ,\quad (i,\ j = 1,\ 2,\ 3)\ , \tag{10}$$

where the tensor $\tilde{\mathbf{\Gamma}}^{(n)}$ is defined by

$$\begin{aligned} \tilde{\Gamma}_{pqrs}^{(4)} &= T_{pq}\,T_{rs}\ , \\ \tilde{\Gamma}_{pqrs}^{(3)} &= V_{pq}\,T_{rs} + T_{pq}\,V_{rs}\ , \\ \tilde{\Gamma}_{pqrs}^{(2)} &= T_{pq}\,Q_{rs} + T_{rs}\,Q_{pq} + V_{pq}\,V_{rs}\ , \\ \tilde{\Gamma}_{pqrs}^{(1)} &= V_{pq}\,Q_{rs} + V_{rs}\,Q_{pq}\ , \\ \tilde{\Gamma}_{pqrs}^{(0)} &= Q_{pq}\,Q_{rs}\ , \end{aligned} \tag{11}$$

and q_n is given by

$$q_n = \begin{cases} \dfrac{-1}{2\beta_1\,\beta_2\,\beta_3}\left[\mathrm{Re}\left\{\displaystyle\sum_{t=1}^{3}\frac{p_t^n}{(p_t - \overline{p}_{t+1})(p_t - \overline{p}_{t+2})}\right\} - \delta_{n2}\right] & \text{for } n = 0, 1, 2\ , \\ \dfrac{1}{2\beta_1\,\beta_2\,\beta_3}\,\mathrm{Re}\left\{\displaystyle\sum_{t=1}^{3}\frac{p_t^{n-2}\,\overline{p}_{t+1}\,\overline{p}_{t+2}}{(p_t - \overline{p}_{t+1})(p_t - \overline{p}_{t+2})}\right\} & \text{for } n = 3, 4\ , \end{cases} \tag{12}$$

where Re{} is the operator to take the real part of a complex variable, and the subscript t follows the cyclic rule $t = (t - 3)$ if $t > 3$. It can be seen that the calculations involved in Eqs. (8) ~ (12) are relatively straightforward and very easy to be programmed into a computer code.

The fundamental solution for tractions T_{ij} can be carried out using

$$T_{ij} = (\sigma_{ik}\,n_k)_j\ , \tag{13}$$

where σ_{ik} is the fundamental solution for stresses at a field point due to a concentrated force applied in the x_j direction at the source point. For computations of the stresses, one needs to determine the strains first and then apply the generalized Hooke's Law. For this purpose, the explicit formulation of $U_{ij,l}$ must also be determined. Using the spherical coordinate system, the unit position vector **y** = **x**/r has components

$$y_1 = \sin\phi\cos\theta\ ,\ y_2 = \sin\phi\sin\theta\ ,\ y_3 = \cos\phi\ . \tag{14}$$

According to the derivations by Lee [2], the derivative of the Green's function for displacements can be expressed as

$$U_{ij,l} = \frac{1}{4\pi^2 r^2}\left[-\pi\, y_l\, H_{ij} + C_{pqrs}\,(y_s M_{lqiprj} + y_q M_{sliprj})\right] , \tag{15}$$

In Eq. (15), the explicit expression of M_{ijklmn} is given in terms of the Stroh's eigenvalue p_t as

$$M_{ijklmn} = \frac{2\pi i}{|\mathbf{T}|^2}\sum_{t=1}^{3}\frac{1}{(p_t - p_{t+1})^2 (p_t - p_{t+2})^2} \left[\Phi'_{ijklmn}(p_t) - 2\Phi_{ijklmn}(p_t)\times\left(\frac{1}{p_t - p_{t+1}} + \frac{1}{p_t - p_{t+2}}\right)\right] , \tag{16}$$

where function $\Phi_{ijklmn}(p)$ is defined by

$$\Phi_{ijklmn}(p) = \frac{\mathrm{B}_{ij}(p)\,\hat{\Gamma}_{kl}(p)\,\hat{\Gamma}_{mn}(p)}{(p-\overline{p}_1)^2 (p-\overline{p}_2)^2 (p-\overline{p}_3)^2} , \tag{17}$$

and $B_{ij}(p)$ is given by

$$\mathrm{B}_{ij}(p) = n_i\, n_j + (n_i\, m_j + m_i\, n_j)\, p + m_i\, m_j\, p^2 . \tag{18}$$

It should be mentioned that this expression becomes invalid when repeated roots of the sextic equation occurs (*i.e.* $p_t = p_{t+1}$ or $p_t = p_{t+1} = p_{t+2}$). A simple way to overcome this problem, extremely rare though, is to introduce a small perturbation to one of the repeated roots.

Although the foregoing formulations are straightforward to be implemented in BEM, a few numerical experiments revealed a couple of drawbacks indeed. Firstly, for the degenerate case of transverse isotropy, computations using single precision shall lead to inaccuracy due to truncation errors. Although this accuracy problem can be rectified using double precision, it will cause computational burden to some extend for complicated and dense meshes. When computational efficiency is concerned, another drawback would be the involving of complex variables. For handling the complex variables, the CPU processing time will double since the programmed code needs to calculate both of the real and the imaginary parts at the same time. The last and the most concerned issue is the use of high-order tensors, especially in the formulations for the displacement derivatives. Our numerical experiments showed that most CPU processing was taken to calculate loops of these tensors, especially with the joined use of double precision. Nevertheless, the formulations are indeed the most explicit for all fundamental solutions existing so far.

4. FUNDAMENTAL SOLUTIONS OF TRANSVERSE ISOTROPY

As aforementioned, there have been lots of fundamental solutions proposed for transverse isotropy in the past. As a matter of fact, transverse isotropy may be treated as a degenerate case of general anisotropy. However, for saving computational costs, the case of transverse isotropy still needs to be treated separately. For the present study, the formulations derived by Pan and Chou [3] are particularly chosen as the subject under investigation. The reason of this choice will be obvious after the formulations are outlined in what follows.

According to what is derived in [3], when point force is applied in the normal direction to the plane of isotropy, provided to be the $x_1 - x_2$ plane herein, the displacements are given by

$$U_{13} = \sum_{i=1}^{2}\left[\nu_i\, A_i\frac{x_1}{R_i\, R_i^*} - \nu_i (A_i + B_i)\frac{x_1\, x_{3i}}{R_i^3}\right] , \tag{19}$$

$$U_{23} = \sum_{i=1}^{2}\left[\nu_i\, A_i\frac{x_2}{R_i\, R_i^*} - \nu_i (A_i + B_i)\frac{x_2\, x_{3i}}{R_i^3}\right] , \tag{20}$$

$$U_{33} = \sum_{i=1}^{2}\left[-\left(\frac{C_{11}\, B_i + C_{44}\,\nu_i^2\, A_i}{C_{13} + C_{44}}\right)\frac{1}{R_i} - \frac{(A_i + B_i)\,\nu_i^2}{C_{13} + C_{44}}\left(\frac{C_{44}\,\rho^2 + C_{11}\, x_3^2}{R_i^3}\right)\right] , \tag{21}$$

where the constants ν_i are defined by

$$\nu_1 = \sqrt{\frac{(\sqrt{C_{11}\, C_{33}} - C_{13})(\sqrt{C_{11}\, C_{33}} + C_{13} + 2C_{44})}{4C_{33}\, C_{44}}} + \sqrt{\frac{(\sqrt{C_{11}\, C_{33}} + C_{13})(\sqrt{C_{11}\, C_{33}} - C_{13} - 2C_{44})}{4C_{33}\, C_{44}}} , \tag{22}$$

$$\nu_2 = \sqrt{\frac{(\sqrt{C_{11}\, C_{33}} - C_{13})(\sqrt{C_{11}\, C_{33}} + C_{13} + 2C_{44})}{4C_{33}\, C_{44}}} - \sqrt{\frac{(\sqrt{C_{11}\, C_{33}} + C_{13})(\sqrt{C_{11}\, C_{33}} - C_{13} - 2C_{44})}{4C_{33}\, C_{44}}} , \tag{23}$$

$$\nu_3 = \sqrt{C_{66} / C_{44}} , \tag{24}$$

and the variables x_{3i}, ρ, R_i, and R_i^* are defined by

$$x_{3i} = \nu_i\, x_3 , \tag{25}$$

$$\rho = \sqrt{x_1^2 + x_2^2} , \tag{26}$$

$$R_i = \sqrt{x_1^2 + x_2^2 + x_{3i}^2} , \tag{27}$$

$$R_i^* = R_i + x_{3i} . \tag{28}$$

The constants A_i and B_i in Eqs. (19) ~ (21) are defined by

$$\nu_1\, A_1 = -\nu_2\, A_2 = \frac{(C_{13} + C_{44})}{4\pi C_{33}\, C_{44}(\nu_2^2 - \nu_1^2)} , \quad B_i = -A_i \ \text{ for } \sqrt{C_{11}\, C_{33}} - C_{13} - 2C_{44} \neq 0 , \tag{29}$$

$$A_1 = A_2 = 0,\ B_1 = B_2 = -\frac{(C_{13}+C_{44})}{16\pi C_{11}\,C_{44}}\ ,$$
$$\text{for } \sqrt{C_{11}\,C_{33}} - C_{13} - 2C_{44} = 0\ . \tag{30}$$

It should be noted that the degenerate case when $\sqrt{C_{11}\,C_{33}} - C_{13} - 2C_{44} = 0$ occurs will lead to $\nu_1 = \nu_2$. Theoretically speaking, this condition $\nu_1 = \nu_2$ will invalidate the computations of A_1 and A_2 if Eq. (29) is used. Numerical experiments showed us a small perturbation will be automatically introduced into the numerical values of ν_1, ν_2 and the constants A_i and B_i can be still calculated using Eq. (29). The advantage of unifying the expressions for the both conditions is that Eq. (29) implies

$$A_i + B_i = 0\ . \tag{31}$$

From Eq. (31), the displacement field of Eqs. (19) ~ (21) can be simplified to

$$U_{13} = \sum_{i=1}^{2} \nu_i\, A_i \frac{x_1}{R_i\, R_i^*}\ , \tag{32}$$

$$U_{23} = \sum_{i=1}^{2} \nu_i\, A_i \frac{x_2}{R_i\, R_i^*}\ , \tag{33}$$

$$U_{33} = \sum_{i=1}^{2} \frac{(C_{11} - C_{44}\,\nu_i^2)A_i}{(C_{13}+C_{44})R_i}\ . \tag{34}$$

As a matter of fact, the fundamental tractions T_{ij} can be directly calculated using the formulations provided [3] for the stresses, namely

$$\sigma_{11} = \sum_{i=1}^{2} \frac{\nu_i\, A_i}{R_i}\left\{\frac{(C_{11} - C_{13}\,\nu_i^2\,k_i)\,z_i}{R_i^2} - \frac{2C_{66}}{R_i^*}\left[1 - \frac{x_2^2}{R_i}\left(\frac{1}{R_i} - \frac{1}{R_i^*}\right)\right]\right\}, \tag{35}$$

$$\sigma_{22} = \sum_{i=1}^{2} \frac{\nu_i\, A_i}{R_i}\left\{\frac{(C_{11} - C_{13}\nu_i^2\,k_i)\,z_i}{R_i^2} - \frac{2C_{66}}{R_i^*}\left[1 - \frac{x_1^2}{R_i}\left(\frac{1}{R_i} - \frac{1}{R_i^*}\right)\right]\right\}, \tag{36}$$

$$\sigma_{33} = \sum_{i=1}^{2} \frac{\nu_i\, A_i\, z_i(C_{13} - C_{33}\,\nu_i^2\,k_i)}{R_i^3}\ , \tag{37}$$

$$\sigma_{12} = -2C_{66}\,x_1\,x_2 \sum_{i=1}^{2} \frac{A_i}{R_i^2 R_i^*}\left(\frac{1}{R_i} + \frac{1}{R_i^*}\right), \tag{38}$$

$$\sigma_{31} = -\frac{C_{44}\,x_1}{C_{13}+C_{44}} \sum_{i=1}^{2} \frac{A_i(C_{11} + C_{13}\,\nu_i^2)}{R_i^3}\ , \tag{39}$$

$$\sigma_{31} = -\frac{C_{44}\,x_2}{C_{13}+C_{44}} \sum_{i=1}^{2} \frac{A_i(C_{11} + C_{13}\,\nu_i^2)}{R_i^3}\ , \tag{40}$$

where k_i and z_i are defined by

$$k_i = \frac{C_{11}/\nu_i^2 - C_{44}}{C_{13}+C_{44}}, \quad z_i = \nu_i\,x_3\ . \tag{41}$$

It should be noted that all the expressions for stresses provided in [3] involving $(A_i + B_i)$ are originally very lengthy. Taking advantage of Eq. (31), these expressions are simplified to Eqs. (35) ~ (40) that are applicable to all conditions no matter it is $\sqrt{C_{11}\,C_{33}} - C_{13} - 2C_{44} = 0$ or $\sqrt{C_{11}\,C_{33}} - C_{13} - 2C_{44} \neq 0$.

When the point force is applied in the direction of x_1-axis, the simplified form of the displacements are determined to be

$$U_{11} = \sum_{i=1}^{2} \frac{2\nu_i\,A_i'}{R_i^*}\left(1 - \frac{x_1^2}{R_i\,R_i^*}\right) + \frac{D}{R_3^*}\left[1 - \frac{x_2^2}{R_3\,R_3^*}\right], \tag{42}$$

$$U_{21} = \sum_{i=1}^{2} -\frac{2\nu_i\,A_i'\,x_1\,x_2}{R_i\,R_i^{*2}} + \frac{Dx_1\,x_2}{R_3\,R_3^{*2}}\ , \tag{43}$$

$$U_{31} = \sum_{i=1}^{2} \frac{A_i'(C_{44}\,\nu_i - C_{11})}{C_{13}+C_{44}} \frac{2x_1}{R_i\,R_i^*}\ , \tag{44}$$

where the constants A_i' and D are defined by

$$A_i' = \frac{(-1)^i(C_{44} - C_{33}\,\nu_i^2)}{8\pi C_{33}\,C_{44}(\nu_1^2 - \nu_2^2)\,\nu_i^2}\ , \tag{45}$$

$$D = \frac{1}{4\pi C_{44}\,\nu_3}\ . \tag{46}$$

In a similar approach of simplification, the expressions for stresses are simplified to have the following forms,

$$\sigma_{11} = \sum_{i=1}^{2} -\frac{2\nu_i\,A_i'\,x_1}{R_i}\left[\frac{C_{44}\,\nu_i^2(1+k_i)}{R_i^2} + \frac{2C_{66}}{R_i^{*2}}\left(-1 + \frac{x_2^2}{R_i^2} + \frac{2x_2^2}{R_i\,R_i^*}\right)\right] + \frac{2C_{66}\,Dx_1}{R_3\,R_3^{*2}}\left(-1 + \frac{x_2^2}{R_3^2} + \frac{2x_2^2}{R_3\,R_3^*}\right), \tag{47}$$

$$\sigma_{22} = \sum_{i=1}^{2} -\frac{2\nu_i\,A_i'\,x_1}{R_i}\left[\frac{C_{44}\,\nu_i^2(1+k_i)}{R_i^2} + \frac{2C_{66}}{R_i^{*2}}\left(-3 + \frac{x_1^2}{R_i^2} + \frac{2x_1^2}{R_i\,R_i^*}\right)\right] - \frac{2C_{66}\,Dx_1}{R_3\,R_3^{*2}}\left(-1 + \frac{x_2^2}{R_3^2} + \frac{2x_2^2}{R_3\,R_3^*}\right), \tag{48}$$

$$\sigma_{33} = \sum_{i=1}^{2} 2(C_{33}\,\nu_i^2\,k_i - C_{13})\ \frac{B_i'\,\nu_i\,x_1}{R_i^3}\ , \tag{49}$$

$$\sigma_{31} = \sum_{i=1}^{2}\left[\frac{2C_{44}\,A'(C_{11i} + C_{13}\,\nu_i^2)}{R_i\,R_i^*\left(C_{13}+C_{44}\right)}\left(1 - \frac{x_1^2}{R_i^2} - \frac{x_1^2}{R_i\,R_i^*}\right)\right] + \frac{C_{44}\,\nu_3 D}{R_3\,R_3^*}\left(-1 + \frac{x_2^2}{R_3^2} + \frac{x_2^2}{R_3 R_3^*}\right), \tag{50}$$

$$\sigma_{32} = \sum_{i=1}^{2} \frac{2C_{44}\,A_i'\,(C_{11} + C_{13}\,\nu_i^2)\,x_1\,x_2}{R_i\,R_i^*(C_{13}+C_{44})}\left(\frac{1}{R_i^2} + \frac{1}{R_i\,R_i^*}\right) - \frac{C_{44}\,\nu_3 Dx_1\,x_2}{R_3\,R_3^*}\left(\frac{1}{R_3^2} + \frac{1}{R_3\,R_3^*}\right), \tag{51}$$

$$\sigma_{12} = \sum_{i=1}^{2} \frac{4C_{66}\,\nu_i\,B_i'\,x_2}{R_i\,R_i^{*2}}\left(-1-\frac{x_1^2}{R_i^2}+\frac{2x_1^2}{R_i\,R_i^*}\right) + \frac{C_{66}\,Dx_2}{R_3\,R_3^{*2}}\left[-2+\frac{(x_2^2-x_1^2)}{R_3^2}+\frac{2(x_2^2-x_1^2)}{R_3\,R_3^*}\right]. \quad (52)$$

It should be noted that Eqs. (49) and (50) have corrected the typographic mistakes in the paper [3]. By interchanging the directions of x_1 and x_2, all the foregoing solutions, provided by Eqs. (42) ~ (44) and (47) ~ (52), can be directly applied to the case when the point force is applied in the direction of x_2-axis,

Up to this point, it is now clear to see the conciseness and straightforwardness of the formulations for transverse isotropy. To the authors' knowledge, they are the most tidy among all solutions proposed so far. As mentioned at the beginning, another advantage of this approach is the applicability to the exact volume-to-surface integral transformation, being demanded for the problem of thermoelasticity. This can be readily achieved if one makes spatial differentiations of U_{ij}, rewrites the differentiated forms in the spherical coordinate system, and determines G_{ijk} by Eq. (4) in the spherical coordinate system. This research is under our way to resolve the 3D thermoelastic problem.

5. NUMERICAL EXAMPLES

In this section, two numerical examples are investigated to verify the veracity and efficiency of all formulations built in an existing computer code, originally established for analysis of isotropic bodies. As shown in Fig. 2, the first example considers a transversely isotropic, linearly elastic solid with its isotropic plane parallel to the $x_1 - x_2$ plane, having the following material constants for its stiffness matrix **C:**

$$\mathbf{C} = \begin{pmatrix} 465 & 124 & 117 & 0 & 0 & 0 \\ 124 & 465 & 117 & 0 & 0 & 0 \\ 117 & 117 & 563 & 0 & 0 & 0 \\ 0 & 0 & 0 & 233 & 0 & 0 \\ 0 & 0 & 0 & 0 & 233 & 0 \\ 0 & 0 & 0 & 0 & 0 & 170.5 \end{pmatrix} \times 10^7\,(\mathrm{N/m^2})\,. \quad (53)$$

Suppose this parallelepiped is subjected to tension $\sigma_o = 1$ (unit) at one end, while the other is constrained according to the exact solution provided by Lenitskii [30]. The BEM mesh employed is shown in Fig. 3, where there are 56 quadrilateral elements with a total of 170 nodes. The displacements, u_i, obtained from the present anisotropic and transversely isotropic analyses at the five points A – G, indicated in Fig. 2, are listed in Table 1. The numerical values are compared with those calculated using Lenitskii's [30] exact solution, where excellent agreement with the exact solution can be seen. To illustrate the efficiencies of computing the fundamental solutions for general isotropy and transverse isotropy, the CPU processing time is analyzed and compared with that of the conventional isotropic

Table 1 Computed displacements compared with exact solution [30]

Point	Disp.	u_1		u_2		u_3	
A (–1, 1, 12)	Exact	0.3845799	Error%	–0.3845799	Error%	23.2324992	Error%
	Aniso	0.3846135	8.74E-3	–0.3845757	1.09E-3	23.2324600	1.69E-4
	Trans.	0.3847809	5.24E-2	–0.3845753	1.20E-3	23.2324962	1.27E-5
B (–1, 0, 10)	Exact	0.3845799	Error%	0.0000000	Error%	19.3604160	Error%
	Aniso	0.3845086	1.85E-2	0.0000007	NA	19.3603187	5.03E-4
	Trans.	0.3846107	8.01E-3	0.0000433	NA	19.3603534	3.23E-4
C (0, 1, 8)	Exact	0.0000000	Error%	–0.3845799	Error%	15.4883328	Error%
	Aniso	–0.0000005	NA	–0.3845450	9.07E-3	15.4882818	3.29E-4
	Trans.	0.0000837	NA	–0.3846219	1.09E-2	15.4882917	2.65E-4
D (0, –1, 6)	Exact	0.0000000	Error%	0.3845799	Error%	11.6162496	Error%
	Aniso	–0.0000002	NA	0.3846496	1.81E-2	11.6161583	7.86E-4
	Trans.	–0.0000259	NA	0.3845615	4.78E-3	11.6161804	5.96E-4
E (1, 1, 4)	Exact	–0.3845799	Error%	–0.3845799	Error%	7.7441664	Error%
	Aniso	–0.3847042	3.23E-2	–0.3843646	5.60E-2	7.7441423	3.11E-4
	Trans.	–0.3845589	5.46E-3	–0.3845769	7.80E-4	7.7441349	4.07E-4
F (–1, –1, 2)	Exact	0.3845799	Error%	0.3845799	Error%	3.8720832	Error%
	Aniso	0.3847161	3.54E-2	0.3845074	1.89E-2	3.8720525	7.93E-4
	Trans.	0.3846086	7.46E-3	0.3845396	1.05E-2	3.8720660	4.44E-4
G (1, 1, 0)	Exact	–0.3845799	Error%	–0.3845799	Error%	0.0000000	Error%
	Aniso	–0.3849127	8.65E-2	–0.3841379	1.15E-1	0.0000000	NA
	Trans.	–0.3846470	1.74E-2	–0.3845047	1.96E-2	0.0000000	NA

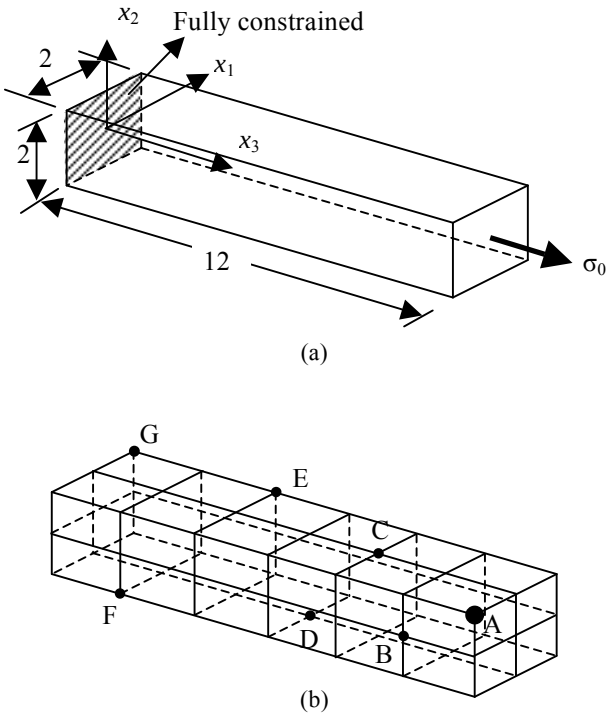

Fig. 2 (a) A parallelepiped subjected to tension; (b) mesh discretization

approach. To see the difference of processing time, 8 × 8 Gauss points are used for the integration of each element. Figure 3 shows the comparison of CPU time taken for all three cases, while the element number is increased from 24 to 104. It is interesting to see that the computational efficiency of the generally anisotropic approach will decline drastically with the increase of element number, while the CPU time for processing transverse isotropy is of the same order of the conventional treatment of isotropy.

The second example considers a cylindrical bar with a spherical cavity under remote tension as depicted in Fig. 4 [13]. The range of cavity sizes considered was $a/R = 0.1$ to 0.5, where a and R are the radii of the cavity and the cylindrical bar, respectively; also, the half-length of the bar $H = 2R$. For illustration of the validity of the simplified formulations for the degenerate condition, the stiffness matrix is assumed to be

$$\mathbf{C} = \begin{pmatrix} 465 & 124 & 124 & 0 & 0 & 0 \\ 124 & 465 & 124 & 0 & 0 & 0 \\ 124 & 124 & 465 & 0 & 0 & 0 \\ 0 & 0 & 0 & 170.5 & 0 & 0 \\ 0 & 0 & 0 & 0 & 170.5 & 0 \\ 0 & 0 & 0 & 0 & 0 & 170.5 \end{pmatrix} \times 10^7 \,(\mathrm{N/m^2}) \tag{54}$$

which shall yield the condition $\sqrt{C_{11}C_{33}} - C_{13} - 2C_{44} = 0$. To demonstrate the difference between transverse isotropy and general anisotropy, the case is also analyzed using the algorithm for anisotropy, where the following stiffness matrix [13] is used

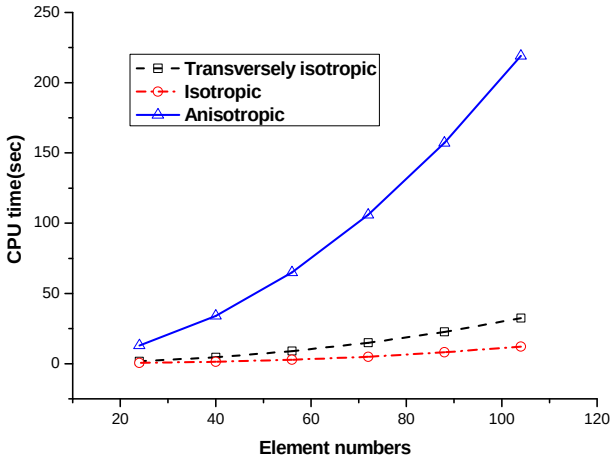

Fig. 3 Comparison of CPU processing time

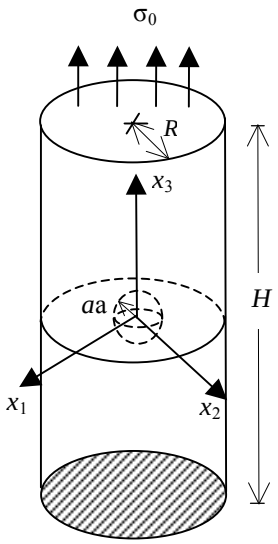

Fig. 4 A cylindrical bar with cavity subjected to tension at one end

$$C = \begin{bmatrix} 544.8 & 153.6 & 57.3 & 10.5 & 65.7 & -81.2 \\ 153.6 & 531.1 & 28.4 & -14.7 & -18.1 & 89.7 \\ 57.3 & 28.4 & 654.4 & 19.8 & -6.4 & 10.4 \\ 10.5 & -14.7 & 19.8 & 106.4 & 24.8 & 13.3 \\ 65.7 & -18.1 & -6.4 & 24.8 & 167.9 & 22.5 \\ -81.2 & 89.7 & 10.4 & 13.3 & 22.5 & 243.5 \end{bmatrix} \times 10^7 \,(\mathrm{N/m^2}) \,. \tag{55}$$

The material properties correspond to an alumina crystal with principal material axes rotated clockwise in the x_1–, x_2– and x_3– directions by 30°, 45° and 60°, respectively. For comparison, finite element analysis is also carried out using ANSYS. Figure 5 shows a typical mesh used for analysis of BEM and ANSYS in all cases of a/R. For the alumina crystal, the computed stress concentration factor, defined by $k_z = \sigma_{33}/\sigma_o$, was found

to be uniform around the horizontal equator of the cavity surface. Figure 6 shows the variation of the stress concentration factor for the various a/R ratios considered. From the figure, excellent agreement between BEM and ANSYS analysis can be observed for the both cases. For the BEM analysis, the CPU processing time for the transversely isotropic case and the generally anisotropic case took 11.5 seconds and 83.4 seconds, respectively. From the view point of computational efficiency, it is apparent to see the necessity of separating the treatment of transverse isotropy from that of anisotropy, although the computation algorithm for treating general anisotropy can certainly deal with transverse isotropy as a special degenerate case.

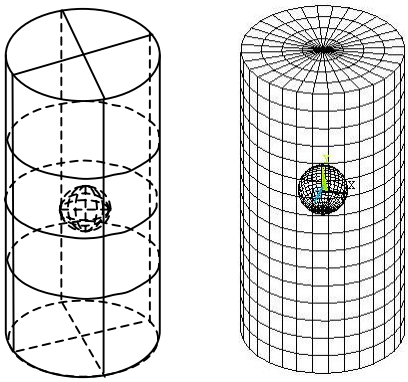

Fig. 5 Mesh discretization used for BEM (left) and ANSYS (right)

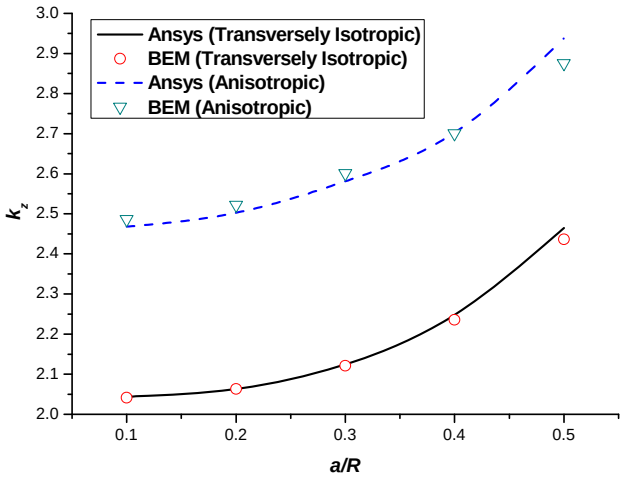

Fig. 6 Stress concentration factors of the spherical cavity in a cylindrical bar

6. CONCLUSIONS

In this article, the 3D fundamental solutions for generally anisotropic [1,2] and transversely isotropic [3] bodies are implemented in BEM and compared with the conventional isotropic approach for the computational efficiency. A few conclusions can be drawn from this investigation. Indeed, the fundamental solutions proposed in [1,2] are very straightforward to be programmed in a computer code; however, the corresponding CPU time will increase greatly for complicated modeling with large amounts of meshes. This is mainly derived from the use of complex variables and high-order tensors. Nevertheless, the formulations themselves still appear to be attracting in form since no special technique is required like the others. When the fundamental solution of transverse isotropy [3] is implemented in BEM, it is found that as expected, the CPU time is comparable with that of the isotropic case. As a matter of fact, this is mainly attributed to the fact the original formulations presented by Pan and Chou [3] can be significantly simplified, yet they are still appropriate for all cases in general. Also, these formulations need to be marked for the potential to treat the associated thermoelastic problem.

ACKNOWLEDGEMENTS

The authors gratefully acknowledge the financial support of the National Science Council of Taiwan, Republic of China (Grant Number: 96-2221-E-035-011-MY3).

REFERENCES

1. Ting, T. C. T. and Lee, V. G., "The Three-Dimensional Elastostatic Green's Function for General Anisotropic Linear Elastic Solid." *Quarterly Journal of Mechanics Applied Mathematics*, **50**, pp. 407–426 (1997).
2. Lee, V. G., "Explicit Expression of Derivatives of Elastic Green's Functions for General Anisotropic Materials," *Mechanics Research Communications*, **30**, pp. 241–249 (2003).
3. Pan, Y. C. and Chou, T. W., "Point Force Solution for an Infinite Transversely Isotropic Solid," *Journal of Applied Mechanics*, **29**, pp. 225–236 (1976).
4. Lifshitz I. M. and L.N. Rozenzweig, L.N., "Construction of the Green Tensor for the Fundamental Equation of Elasticity Theory in the Case of Unbounded Elastically Anisotropic Medium," *Journal of Experimental and Theoretical Physics*, **17**, pp. 783–791 (1947).
5. Synge, J. L., *The Hypercircle in Mathematical Physics*, Cambridge University Press, Cambridge (1957).
6. Barnett, D. M., "The Precise Evaluation of Derivatives of the Anisotropic Elastic Green's Functions," *Physica Status Solidi*, (b) **49**, pp. 741–748 (1972).
7. Wilson, R. B. and Cruse, T. A., "Efficient Implementation of Anisotropic Three Dimensional Boundary Integral Equation Stress Analysis," *International Journal for Numerical Methods in Engineering*, **12**, pp. 1383–1397 (1978).
8. Chen, T. and Lin, F. Z., "Numerical Evaluation of Derivatives of the Anisotropic Elastic Green's Functions," *Mechanics Research Communications*, **20**, pp. 501–506 (2001).

9. Nakamura, G. and Tanuma, K., "A formula for the Fundamental Solution of Anisotropic Elasticity," *Quarterly Journal of Mechanics Applied Mathematics*, **50**, pp. 179–194 (1997).
10. Wang, C. Y., "Elastic Fields Produced by a Point Source in Solids of General Anisotropy," *Journal of Engineering Mathematics,* **32**, pp. 41–52 (1997).
11. Tonon, F., Pan, E. and Amadei, B., "Green's Functions and Boundary Element Method Formulation for 3D Anisotropic Media," *Composite and Structures*, **79**, pp. 469–482 (2001).
12. Wang, C. Y. and Denda, M., "3D BEM for General Anisotropic Elasticity," *International Journal of Solids and Structures,* **44**, pp. 7073–7091 (2007).
13. Tan, C. L., Shiah, Y. C. and Lin, C. W., "Stress Analysis of 3D Generally Anisotropic Elastic Solids Using the Boundary Element Method," *CMES-Computer Modeling in Engineering and Sciences*, **41**, pp. 159–214 (2009).
14. Eubanks, R. A. and Sternberg, E., "On the Axisymmetric Problem of Elasticity Theory for a Medium with Transverse Isotropy," *Journal of Rational Mechanics and Analysis,* **3**, pp. 89–101 (1954).
15. Gurtin, M. E., The linear theory of elasticity, in: S. Flugge, C. Truesdell Eds., Handbuch der Physik, *Mechanics of Solids II,* Via/2, Springer, Berlin, pp. 1–295 (1972).
16. Michell, J. H., "The Stress in an Anisotropic Elastic Solid with an Infinite Plane Boundary," *Proceedings London Mathematics Society,* **32**, pp. 247–258 (1900).
17. Hu, H. C. "On the Three Dimensional Problems of the Theory of Elasticity of a Transversely Isotropic Body," *Society Sinica,* **2**, pp. 145–151 (1953).
18. Nowacki, W., "The Stress Function in Three-Dimensional Problems Concerning an Elastic Body Characterized by Transverse Isotropy," *Bulletin De L'Acadbmie Polonaise Des Sciences,* **4**, pp. 21–25 (1954).
19. Lodge, A. S., "The Transformation to Isotropic form of the Equilibrium Equations for a Class of Anisotropic Elastic Solids," *Quarterly Journal of Mechanics Applied Mathematics*, **8**, pp. 211–225 (1955).
20. Alexsandrov, I. Y. and Soloviev, U. I., *Three-Dimensional Problems of Elastic Theory*. Science, Moscow (1978).
21. Ding, H. J. and Xu, B. H., "General Solutions of Axisymmetric Problems in Transversely Isotropic Body," *Applied Mathematics Mechanics*, **9**, pp. 135–142 (1988).
22. Horgan, C. O. and Simmonds, J. G., "Asymptotic Analysis of an End-Loaded, Transversely Isotropic, Elastic, Semi-Infinite Strip Weak in Shear," *International Journal of Solids and Structures*, **27**, pp. 1895–1914 (1991).
23. Wang, M. Z. and Wang, W., "Completeness and Non-uniqueness of General Solutions of Transversely Isotropic Elasticity," *International Journal of Solids and Structures*, **32**, pp. 501–513 (1995).
24. Fabrikant, V. I., "Complete Solution to the Problem of an External Circular Crack in a Transversely Isotropic Body Subjected to Arbitrary Shear Loading," *International Journal of Solids and Structures*, **33**, pp. 167–191 (1996).
25. Tarn, J.-Q. and Wang, Y.-M., "A Fundamental Solution for a Transversely Isotropic Elastic Space," *Journal of the Chinese Institute of Engineers*, **10**, pp. 13–21 (1987).
26. Chen, J. T., Liao, H. Z. and Lee, W. M., "An Analytical Approach for the Green's Functions of Biharmonic Problems with Circular and Annular Domains," *Journal of Mechanics*, **25**, pp. 59–74 (2009).
27. Shiah, Y. C., Lin, Y.-S. and Chen, Y. H., "Analysis for Thermal Conductance Effect on the Interfacial Thermal Stresses of Anisotropic Composites," *Journal of Thermal Stresses*, **31**, pp. 991–1005 (2008).
28. Hong, H.-K. and Chen, J. T., "Derivations of Integral Equations of Elasticity," *Journal of Engineering Mechanics*, ASCE, **114**, pp. 1028–1044 (1988).
29. Rizzo, F. J. and Shippy, D. J., "An Advanced Boundary Integral Equation Method for Three-Dimensional Thermoelasticity," *International Journal of Numerical Methods Engineering*, **11**, pp. 1753–1768 (1977).
30. Lenitskii, S. G., *Theory of Elasticity of an Anisotropic Body*. Holden-Day, San Francisco (1963).

(Manuscript received September 30, 2009,
accepted for publication January 29, 2010.)